SKIN-ELECTRODE IMPEDANCE MODEL FOR TYPICAL TRANSCUTANEOUS ELECTRICAL STIMULATION PULSES

José Luis Vargas Luna[1,2], Matthias Krenn[2], Jorge Armando Cortés Ramírez[1] and Winfried Mayr[2]
[1]Centro de Innovación en Diseño y Tecnología, Tecnológico de Monterrey
Av. Eugenio Garza Sada Sur 2501, Tecnológico, 64849 Monterrey, Nuevo León, Mexico
[2]Center for Medical Physics and Biomedical Engineering, Medical University of Vienna
Währinger Gürtel 18-20/4L, A-1090 Vienna, Austria
Email: joseluis.vargasluna@gmail.com

ABSTRACT
A new model for the skin-electrode interface impedance is presented. This model is developed to work with typical Transcutaneous Electrical Stimulation (TES) parameters and, unlike other models, is able to predict low and high charge pulses since it considers the electroporation and a charge-dependent effect. Experimental data are acquired with Current-Control (CC) and Voltage-Control (VC) stimulation pulses. The data show a predominant current-dependency for both stimulation techniques, which allows to keep a simple model. A computational simulation is run with biphasic pulses of CC and VC, getting R^2-values up to 0.99. The model can be fitted for each electrode type with few experimental points, and be easily embedded in optimization algorithms to design new pulse waveforms and study of high-charges pulses of actual TES techniques.

KEY WORDS
Skin-Electrode Impedance, Model, Functional Electrical Stimulation (FES), Current-Control, Voltage-Control.

1. Introduction

Transcutaneous Electrical Stimulation (TES) is a powerful tool for diagnosis, research, treatment and function restoration. Depending on the approach Current-Control (CC) or Voltage-Control (VC) devices can be used [1].
Many studies have reported spectroscopy measurements of the tissue-electrode impedance, deriving in some mathematical models [2]–[4]. However, spectroscopy uses sinusoidal current injection for modeling, which is non-common on electrical stimulation. Typical TES therapies use rectangular or triangular pulses (in all their variations) at relatively low frequencies (<50Hz), and pulse widths of <2000μs for innervated muscles [5] and <100ms for denervated muscles [6]. Few studies are found to understand impedance dynamics under TES but most of them only consider low-charges pulses [7]. It has been reported that current-voltage response in long pulses exhibits a different behavior to the one expected in conventional models based on RC networks [8].
The understanding of the skin-electrode interface impedance and the ability to predict its behavior under typical TES conditions is important, since previous studies indicate that the impedance also plays an important role into the performance and controllability of both CC and VC stimulation [9]. Moreover, new approaches for selective stimulation are based in the design of stimulation waveforms. For example, it had been reported that the use of depolarizing pre-pulses (DPP) reduce fiber excitability, while hyperpolarizing pre-pulses (HPP) increase it [1]. Pulse shapes that include such pre-pulses work in both low intensities and high intensities, therefore understand the different mechanisms present in the skin-electrode interface could be a key feature for device and waveform design.
This work presents a model of skin-electrode interface impedance that works with typical TES pulses, which is able to deal with low and high pulse charges. The mathematical model is adjusted with experimental data applying biphasic rectangular waves in both CC and VC. A validation is done using dynamic simulations.

1.1 Skin Anatomy

The skin is a complex structure but is essentially composed by two layers: the epidermis (outer layer) and a dermis. They can vary in thickness depending on the zone, going from 1mm at the eyelid up to more than 1cm in the foot. The density of secondary structures like follicles, sweat glands, oil glands and sensory nerves, also may vary from place to place.
The epidermis is composed by a lipid-corneocyte matrix arranged in a flattened and irregular fashion, which is crossed by skin appendages (*e.g.* sweat glands and hair follicles) [10]. The outer layer of the epidermis is called *stratum corneum* (SC) and is composed by a lipid lamellae-corneocyte matrix arranged in bilayers (between 25 and 100), and has an approximate thickness between 10 to 100μm [11], [12]. Since the films are weakly bonded, they may flaking away and be easily removed, therefore its number may vary [13].
It is documented that the body impedance suffer non-linear variations during TES [14], which are mainly attributed to the skin-electrode interface. Some studies

DOI: 10.2316/J.2014.216.818-0016

have localized this phenomenon in the *stratum corneum* [15], and showed an important reduction of such variability when the SC is removed.
There are at least two pathways for ionic flow into the SC: The first one that goes between the stratification of the SC layers; and a second one that goes through the appendages, mainly the sweat macropores (Fig. 1). It has been shown that most of the ionic movement happens in the sweat pores, since the sweat is an electrolytic fluid and highly conductive [16].

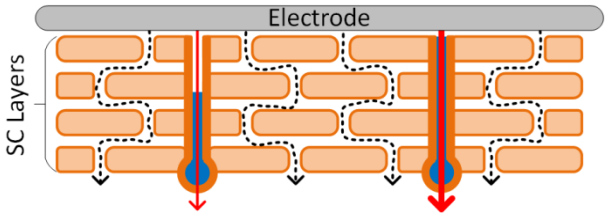

Fig. 1. Simplify model of the *Stratum Corneum* and its ionic pathways. Appendage's ionic pathways (hard line) and pathways going between the stratification of the SC layers (dotted line). Adapted from [2], [4], [16].

1.2 Impedance Variation Mechanisms

There are many theories that try to explain the mechanisms that underlay the impedance variations on the skin. In a general sense, such theories can be grouped according to the speed of the mechanisms that describe: instantaneous changes (within few microseconds [10], [12]) and progressive changes (from milliseconds to hours [2], [15], [17]).
The instantaneous changes are commonly addressed to the electroporation of the skin that is the phenomenon in which the membrane's permeability to ions and macromolecules is increased by exposing it to a high electrical field [18]. For TES, the electroporation process occurs in both ionic pathways, but at low amplitudes just the macropores are affected [11].
While instantaneous impedance variations have been widely investigated, there is still controversy about which is the mechanism of the slow changes. The most extended studies show that progressive increase of ions in the interface could be the answer [2], [4], [17]. Almasi & Schmitt established that the decreasing of impedance in long term applications is because the skin below the electrode gets more hydrated or wet. This is due to the natural diffusion of ions and the expelled sweat that remains trapped below the electrode [17]. However these mechanisms work in the time scale of seconds up to hours and cannot explain the non-exponential behavior of the impedance within the electrical pulses duration (up to 100ms for denerved muscles). Grimnes and collaborators have proposed the electro-osmosis and/or electrophoresis as mechanisms for filling the sweat conducts [2], [4]. Both mechanisms are more suitable to explain the impedance variations within the stimulus' duration, since they start to work instantaneously and changes along the stimulation pulse depending on the injected charge and speed of ions. The impedance variation due to the filling of sweat-pores is represented in Fig. 1, where bigger currents cross through the completely filled ducts than in the semi-filled ducts.

2. Methodology

In order to understand the impedance variation with typical TES parameters, it was necessary to develop a mathematical model that takes into account the known mechanisms and at same time, it was easy to implement in simulations. Afterwards, an experimental setup was defined in order to acquire the necessary data to calculate the model's variables for a specific setup. Finally, the model was validated with different pulses into a simulation and the accuracy was discussed.
The whole model was done based on two assumptions:

- The electroporation effect is instantaneous, since the transient (few microseconds) cannot be detected at the sampling rate used.
- The impedance of the deep-tissue and the bulk solution of the electrode remain constant for each subject.

2.1 Mathematical Model

Due to the complexity of the skin-electrode interface impedance, measurements cannot be done directly. Instead, an equivalent RC-network model can be used and tuned to describe the measured current-voltage response [14]. Based on the skin anatomy and the impedance variation mechanisms, the model shown in Fig. 2 is proposed as a suitable equivalent RC network. On it, the charge-dependent effect, R_o (presumably electro-osmosis), is introduced in series with the electroporation effect (R_e). R_o goes from an initial value (given for the skin conditions) down to zero, when the skin is completely humid.

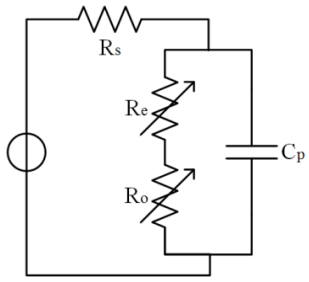

Fig. 2. Proposed skin-electrode interface model.

R_e behavior is commonly represented with a decreasing exponential form [14]. However, the physical phenomenon that describes R_e is an increase of the medium conductance. This is consistent with preliminary data, which suggest that R_e can actually be modeled with the linear behavior of its conductance G_e (Eq. (1)).

$$R_e=\frac{1}{G_e}$$
$$G_e(A)=a_eS(t)+b_e \quad (1)$$

Where *S(t)* represent the stimulation current at a given time (*t*); b_e represents the conductance at no excitation (*S*=0mA); and a_e defines the conductance increase with respect to the current.

On the other hand, the charge-dependent effect (R_o) could be modeled with the next proposed equations:

$$R_o=\begin{cases} R_{oi} & ,Ch<Ch_{th} \\ R_{oi}\left(1-\frac{1}{1+\frac{a_o}{Ch(t)-Ch_{th}}}\right) & ,Ch\geq Ch_{th} \end{cases} \quad (3)$$

$$R_{oi}=R_p(t=0)-R_e \quad (4)$$

$$Ch=\int |i(t)|dt \quad (5)$$

$$a_o=a_aI(t)+b_a \quad (6)$$

Where R_{oi} is the initial value of the resistance, which depends on the skin conditions; Ch_{th} is the charge (in [C]) threshold where the electro-osmotic effect starts to be relevant (inflexion point); Ch(t) represents the charge of the pulse at time *t* and; a_o represent the variation of the medium's (where the ions are moving) electric properties due to electroporation.

The equivalent RC model shown in Fig. 2 follows, under typical conditions, the step response described by Eq. (7) and (8) for CC and VC respectively[19].

$$v(t)=i(t)R_s+i(t)R_p\left(1-e^{-\frac{t}{R_pC}}\right) \quad (7)$$

$$i(t)=\frac{v(t)}{R_s+R_p}-\left(\frac{v(t)}{R_s+R_p}-\frac{v(t)}{R_s}\right)e^{-\frac{t}{(R_s\|R_p)C}} \quad (8)$$

$$R_p=R_e+R_o \quad (9)$$

For both cases, the evaluation of the voltage-current response at *t*=0 reflects the value of R_s, because the capacitor acts as short-circuit. On the other hand, the final stable value corresponds to the effect of R_s and R_p, because a fully-charged capacitor behaves as open circuit. Notice also that in Eq. (9) R_o tends to zero after a given charge, therefore, if enough charge is applied (*e.g.* at the end of the pulse) the signal tends to stabilize and R_p will only depict the value of R_e.

2.2 Experimental Setup

Measurements in 3 neuromuscular intact volunteers were done. The protocol was run in both legs (subjects) of each volunteer. CC and VC stimulation were applied using commercial self-adhesive hydrogel electrodes (SN-50900, Hivox Biotek Inc., Taiwan) of 5x10cm. For both stimulation types the stimulator STMISOLA (Biopac Systems, Inc., USA) controlled with a NI MyDAQ card (National Instruments Corp., USA) was used. The TES was applied on the anterior thigh (anodic electrode in proximal and cathodic electrode in distal side) with an inter-electrode distance of 10cm. A custom code was implemented in LabVIEW™ 2012 (National Instruments, Corp., USA) for the control of the stimulator (100kHz) and the acquisition of the voltage-current response (at 150kS/s).

The whole protocol used charge-balanced biphasic rectangular pulses, and consisted of two stages: (1) CC stimulation and, (2) VC stimulation. The stimulation sweeps were done at 30,000µs/phase and varied from 1mA or V (in steps of 1mA or 1V) up to the pain threshold of the subject or the current limit of the stimulator (110mA).

2.3 Data Processing

The data were post-processed in MATLAB® (The MathWorks, Inc., USA). The acquired data were filtered with a moving average filter (span=5) and an offset extraction in both signals was performed. Afterward, four time metrics were calculated (Fig. 3):

- Beginning of the pulse (t_{i1}): for CC, it is the first current sample equal or greater than the 98% of the pulse amplitude. For VC it is the current sample with biggest value.
- End of first phase (t_{f1}): It is the first sample (after the beginning) in fall below the 99% of the pulse amplitude.
- End of second phase (t_{f2}): It is the last current sample (after the end of first phase) below -99% of the pulse amplitude.
- Inflexion point (t_m): It is the point where the electro-osmotic effect starts to be relevant and the system depicts a different behavior to the one of a RC circuit; this is the time at which the pulse reaches Ch_{th}.

According to the mathematical model, R_s and R_e were calculated from the apparent impedance at t_{i1} and t_{f2} (if stability is reached) respectively. The applied charge to points t_m, t_{f1} and t_{f2} was calculated with Eq. (10). Finally, C and R_p were estimated, with the Eq. (7) and (8), using the time segments where the applied charge is below Ch_{th}.

$$Ch=\sum_{t=0}^{t=t_m;t_{f1};t_{f2}}|i(t)|T_s \quad (10)$$

In order to validate the model, a virtual bench was developed on Simulink® (The MathWorks, Inc., USA). While the model is based mainly on the first phase of the pulse, the simulation was done with the whole pulse. The R^2 and MSE values for the simulation were calculated.

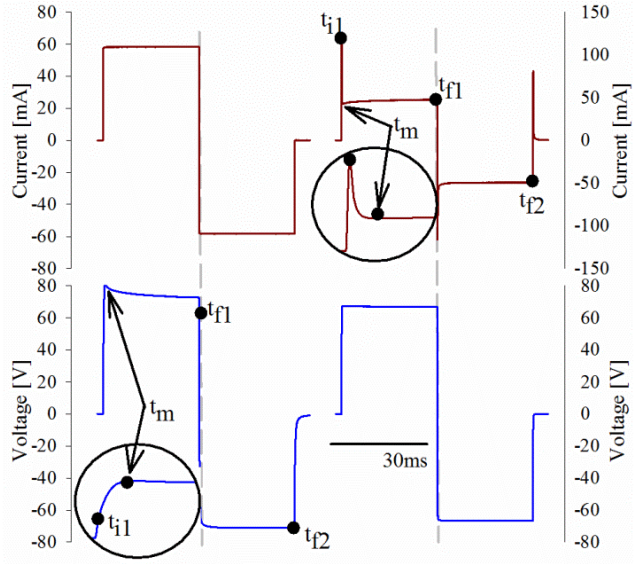

Fig. 3. Typical current-voltage response for CC (left) and VC (rigth) for 30ms pulses. A detail of the first 12ms is displayed for better appreciation of the inflexion point and the beginning of the pulse.

3. Results

The values of R_s remain quasi-stable along the whole stimulation amplitudes. A slight decreasing trend is observed for some cases, however, within the stimulation ranges, this decrease can be neglected. Table 1 presents the values for each stimulation type (Mean±std).

Table 1
Summary of the values of R_s and C

Parameter	Stimulation type	Values
R_s	Current-Control	496±95Ω
	Voltage-Control	441±65Ω
C	Current-Control	238±62nF
	Voltage-Control	224±63nF

Fig. 4 shows the typical G_e data for both stimulation types, as well as the model described in Eq. (1). Table 2 shows the average values of the coefficients for G_e estimation, and the R^2 of the fitting.

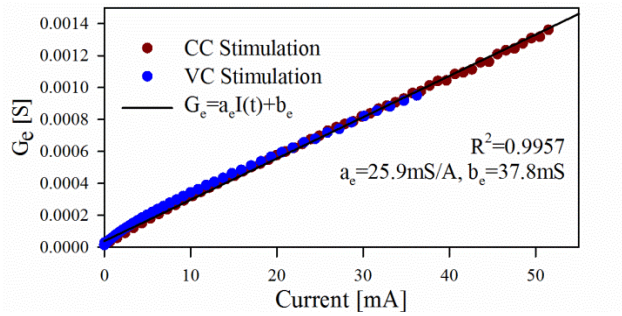

Fig. 4. Typical estimated G_e values as function of the current.

Table 2
Summary of values for estimate G_e and G_p

Coefficient		Mean±std	Range
G_e	a_e	25±2mS/A	21-28mS/A
	b_e	65±29µS/A	28-96µS/A
	R^2	0.982	0.961-0.996
G_p	a_p	15±3.3mS/A	11-19mS/A
	b_p	50±27µS	10-75µS
	R^2	0.949	0.911-0.982

The inflexion point was easily detected on VC pulses, where the charge increases slowly and the charge-dependent decreasing effect (of the impedance) could be progressively observed. Once the effect appeared, the inflexion point was estimated as Ch_{th}=20.1µC. For CC, the measurement is not that clear, since the increase on charge is much faster and only one measurement per subject (at 1mA) does not show the charge-dependent effect.

Once the beginning of the charge-dependent effect was defined, an estimation of the current-voltage response was done, with the data preceding the Ch_{th}, based on Eq. (7) and Eq. (8). Such estimation provides the C values shown in Table 1.

In the same way that G_e, G_p model is based on its current dependency (Fig. 5). It is important to notice that for VC stimulation it was consider the current value at the steady state. The coefficients for estimate G_p are shown in Table 2. Then, with a proper estimation of G_e and G_p, R_{oi} is calculated based on Eq. (4).

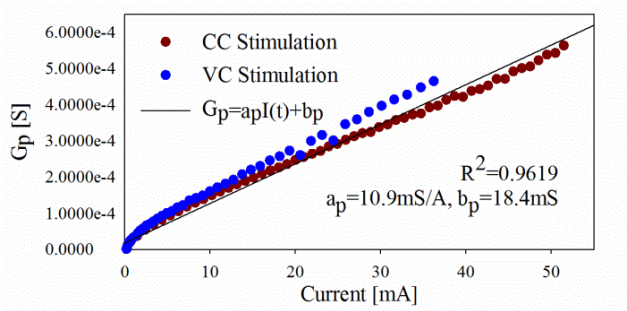

Fig. 5. Typical estimated G_p values as function of the current.

In order to model a_o, it was adjusted for different CC stimulation levels, and then fitted with a linear regression. All the coefficient values for subject 9 (who is used as example in all the figures) are shown in Table 3.

A simulation was done for all pulses in CC and VC stimulation. The results for some of them are shown in Fig. 6, it is also presented the mean square error (MSE) and R^2 for each pulse.

Table 3
Coefficient values for Subject 9

Symbol	Value	Units
Rs	CC:387,VC:356	Ω
C	CC:269,VC:259	nF
Ch_{th}	17.5	µC
a_p	10.9	mS/A
b_p	18.4	µS
a_e	25.9	mS/A
b_e	37.8	µS
a_a	200	µC/A
b_a	3.5	µC

4. Discussion

As expected, R_s values are stable along the whole stimulation range. However, slight differences between the values estimated for CC and VC are noticed. It is possible that the measured differences are because it is assumed an ideal step pulse. For this reason, especially for CC, the selection of the initial time could include the capacitance's charging period. In general, values differ between subjects, but all of them are in the same range.
R_e is effectively estimated with the linear model in the applied stimulation range. It is found that the coefficient values can be applied for both stimulation types, which means that the assumption of current-dependency is acceptable. It is important to notice that in some point G_e must saturate; however, in the applied stimulation range, such effect cannot be appreciated or estimated.

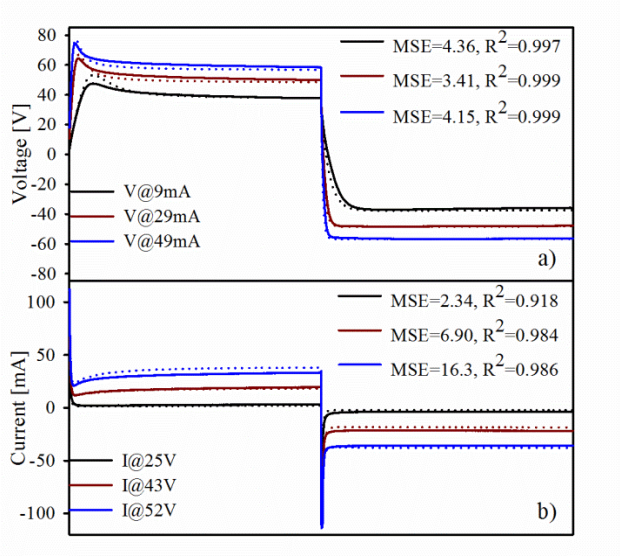

Fig. 6. Typical results from the simulation of the model for a) CC stimulation and, b) VC stimulation. Measured values (hardline) and simulation result (dotted line).

The Ch_{th} is fixed to 17.5µC for all the subjects. This value is chosen because at the highest amplitudes, it is expected that at the detected inflexion point, the charge dependent effect is already started, but it is not seen because of the huge current peak dynamic.
The capacitance is modeled as a constant within the stimulation ranges. As in R_s, a slight decreasing trend is observed for some cases. However, within the stimulation ranges this phenomenon can be neglected, since no relevant improvement is obtained in the final model accuracy.
The linear model of R_p has a good fit within the stimulation ranges and, as in R_e, the model cannot be extrapolated since the value of the conductance (G_p) must saturate in some point, which cannot be defined with the actual setup. However, the model covers most of the clinically accepted amplitudes, since in most cases, the stimulation was applied until volunteers could not stand higher amplitudes due to pain threshold was reached.
The coefficient a_o is adjusted in order to give more weight to the beginning of each phase (and not the saturated values at the end).
Although the model is based mainly on the first phase, the dynamic simulation shows that it is able to predict the impedance behavior during the whole biphasic pulse with CC and VC stimulation. The R^2 and MSE remain in acceptable levels in CC while in VC such parameters are slightly degraded because of small mismatches of the saturation levels.

5. Conclusion

The proposed model is able to predict the skin-electrode interface impedance for both stimulation types (CC and VC). The mathematic model is based on the anatomical structure of the interface and all the variables represent a biological phenomenon or structure.
The whole model is based on nine variables. All variables can be calculated with a single sweep of stimulation amplitudes and work in both stimulation types. It is important to notice that G_e, G_p and a_o are modeled with a linear behavior, therefore, only few points are required for its calculation, while R_s, C and Ch_{th} require (essentially) only one point.
Unlike other works found in literature, this model is developed using typical stimulation parameters for clinical applications of transcutaneous electrical stimulation: pulse waveform, stimulation ranges and duration. In the last case, although the long durations used are mainly employed for denervated muscles, the impedance behavior for shorter pulses is identical to the beginning of the used pulses.
The whole model is current-based, and can be dynamically adjusted. This allows the model to predict the current-voltage response for any shape and, therefore, evaluate or optimize the performance of new pulse waveforms.

References

[1] W. M. Grill and J. T. Mortimer, "Stimulus waveforms for selective neural stimulation," *IEEE Eng. Med. Biol. Mag.*, vol. 14, no. 4, pp. 375–385, 1995.

[2] S. Grimnes, "Skin impedance and electro-osmosis in the human epidermis," *Med. Biol. Eng. Comput.*, vol. 21, no. 6, pp. 739–749, Nov. 1983.

[3] H. P. Schwan, "ELECTRODE POLARIZATION IMPEDANCE AND MEASUREMENTS IN BIOLOGICAL MATERIALS," *Ann. N. Y. Acad. Sci.*, vol. 148, no. 1 Bioelectrodes, pp. 191–209, Feb. 1968.

[4] G. K. Johnsen, C. a. Lütken, Ø. G. Martinsen, and S. Grimnes, "Memristive model of electro-osmosis in skin," *Phys. Rev. E*, vol. 83, no. 3, p. 031916, Mar. 2011.

[5] M. Krenn, M. Haller, M. Bijak, E. Unger, C. Hofer, H. Kern, and W. Mayr, "Safe neuromuscular electrical stimulator designed for the elderly.," *Artif. Organs*, vol. 35, no. 3, pp. 253–6, Mar. 2011.

[6] C. Hofer, W. Mayr, H. Stöhr, E. Unger, and H. Kern, "A stimulator for functional activation of denervated muscles.," *Artif. Organs*, vol. 26, no. 3, pp. 276–9, Mar. 2002.

[7] G. Kantor, G. Alon, and H. S. Ho, "Simulated tissue loads for testing of transcutaneous electrical stimulators," in *Proceedings of 16th Annual International Conference of the IEEE EMBS*, 1994, pp. 784–785.

[8] S. J. Dorgan and R. B. Reilly, "A model for human skin impedance during surface functional neuromuscular stimulation.," *IEEE Trans. Rehabil. Eng.*, vol. 7, no. 3, pp. 341–8, Sep. 1999.

[9] J. L. Vargas Luna, M. Krenn, J. A. Cortés, and W. Mayr, "Comparison of Current and Voltage Control Techniques for Neuromuscular Electrical Stimulation in the Anterior Thigh.," *Biomed. Tech. (Berl).*, Sep. 2013.

[10] Y. A. Chizmadzhev, V. G. Zarnitsin, J. C. Weaver, and R. O. Potts, "Mechanism of electroinduced ionic species transport through a multilamellar lipid system.," *Biophys. J.*, vol. 68, no. 3, pp. 749–65, Mar. 1995.

[11] Y. A. Chizmadzhev, A. V Indenbom, P. I. Kuzmin, S. V Galichenko, J. C. Weaver, and R. O. Potts, "Electrical properties of skin at moderate voltages: contribution of appendageal macropores.," *Biophys. J.*, vol. 74, no. 2 Pt 1, pp. 843–56, Feb. 1998.

[12] U. Pliquett, R. Langer, and J. C. Weaver, "Changes in the passive electrical properties of human stratum corneum due to electroporation," *Biochim. Biophys. Acta - Biomembr.*, vol. 1239, no. 2, pp. 111–121, Nov. 1995.

[13] J. P. Reilly, *Electrical Stimulation and Electropathology*, 1st. Editi. New York, USA: Cambridge University Press, 1992.

[14] T. Keller and A. Kuhn, "Electrodes for transcutaneous (surface) electrical stimulation," *J. Autom. Control*, vol. 18, no. 2, pp. 35–45, 2008.

[15] S. J. Dorgan and R. B. Reilly, "A model for human skin impedance during surface functional neuromuscular stimulation.," *IEEE Trans. Rehabil. Eng.*, vol. 7, no. 3, pp. 341–8, Sep. 1999.

[16] S. Grimnes, "Pathways of ionic flow through human skin in vivo.," *Acta Derm. Venereol.*, vol. 64, no. 2, pp. 93–8, Jan. 1984.

[17] J. J. Almasi and O. H. Schmitt, "SYSTEMIC AND RANDOM VARIATIONS OF ECG ELECTRODE SYSTEM IMPEDANCE," *Ann. N. Y. Acad. Sci.*, vol. 170, no. 2 International, pp. 509–519, Jul. 1970.

[18] A. Ivorra, "Tissue electroporation as a bioelectric phenomenon: Basic concepts," in *Irreversible Electroporation*, B. Rubinsky, Ed. Springer Berlin Heidelberg, 2010, pp. 23–61.

[19] T. H. Glisson, *Introduction to Circuit Analysis and Design*. Dordrecht: Springer Netherlands, 2011.